RESEARCH ARTICLE

Preparation of PVA/tetra-ZnO composite with framework-supported pore-channel structure and the removal research of lead ions

Sheng Xu[1] · Xinde Jiang[1] · Lingli Liu[1] · Zhenxi Wang[1] · Xiaohang Zhang[1] · Yong Peng[1] · Meng Cao[1]

Abstract

Polyvinyl alcohol (PVA) filled with different kinds of ZnO whisker was prepared by chemical cross-linking reaction. It was found that the ZnO whiskers dispersed uniformly after being modified by 3-aminopropyltriethoxysilane (APTES). The PVA/tetrapod-shaped ZnO (PVA/tetra-ZnO) composites showed better adsorption performance than other kinds of PVA/ZnO composites. The framework-supported pore-channel structure was beneficial for the transmission and adsorption of heavy metal ions, and the formation of "brush" pore-channel of PVA/tetra-ZnO composites can effectively retain and capture the heavy metal ions. The PVA/tetra-ZnO composites presented well adsorption on Pb(II), Cd(II), and Cr(III) ions than Ni(II) and showed relatively selective removal on Pb(II) and Cr(III) ions. The adsorbed heavy metal ions presented gradient distribution with high content in the out layer and low content in the inner layer. Pb(II) adsorption capacity q_e increased gradually with the increase of initial solution concentration and contact time which tended to be stable at 400 mg/L and 800 min. The maximal adsorption capacity q_m obtained by nonlinear fitting reached to about 116 mg/g which was very close to the experiment data. Adsorption isotherm results indicated the monolayer adsorption process of the Langmuir model and the adsorption kinetics data fitted well to the pseudo-second-order model. The adsorption process was spontaneous and the high temperature was in favor of adsorption. The adsorption mechanism was explored as the combination of coordination and ion exchange. Besides, the PVA/tetra-ZnO composites exhibited better stress stability, thermo stability, and favorable regeneration than neat PVA.

Keywords "Framework support" structure · Tetrapod-shaped whiskers · Heavy metal ions · Adsorption performance · Stress stability · Regeneration

Introduction

Water is a kind of precious and non-renewable resource which is the concern of all life including humans, animals, and plants. However, the water has been polluted by various organic and inorganic pollutants seriously in recent years (Abdullah et al. 2019; Ahmed et al. 2017; Sarma et al. 2019). Among which, the pollution of heavy metal ions contributes the most harm to the environment, such as the Ni(II), Cd(II), Cr(III), and Pb(II) ions (Abdelrahman and Hegazey, 2019; Tran and Chao, 2018; Reddi et al. 2015; Li et al. 2018). Researches show that the heavy metal ion is harmful to human organs and the heavy metals in wastewater will not degrade in the environment (Liu et al. 2019; Arshad et al. 2019; Huang et al. 2018). Therefore, the study and development of a reliable technique for the removal of heavy metal ions in the environment is significant. Among the numerous methods, the chemical adsorption is an available technique due to its high efficiency, easy operation, and high regeneration ability. Therefore, many materials have been studied to evaluate the removal of heavy metal, such as activated carbon (Ko et al. 2018), scheelite (Dong et al. 2019), carbon nanofibers (Chen et al. 2018), magnetic bentonite (Zou et al. 2019), and PAMAM/CNT (Hayati et al. 2018). However, these nano or powder-type adsorbents are complicated in prior processing and present high cost and some other disadvantages, especially, they are difficult to

---

✉ Zhenxi Wang
wangzhenxi1978@126.com

[1] College of Sciences, Nanchang Institute of Technology, Nanchang 330099, China

recycle in flowing water system and easy to cause secondary pollution. Hence, it is necessary to seek a new adsorbent with high efficiency, low cost, and good recyclability.

Three-dimensional network-structured poly(vinyl alcohol) (PVA) gel with good biocompatibility, non-toxicity, and low cost presents favorable prospect in wastewater treatment and has attracted great attention. Hui et al. (2015) studied the structure of PVA/gelatin hydrogel beads and researched the adsorption mechanism for Pb(II) removal, the result indicated that the introduction of gelatin increased the pore size of PVA and enhanced the adsorption capacity with the coordination between the carboxyl groups and Pb(II) ions. Ajitha et al. (2017) successfully prepared chitosan oligosaccharide-graft-maleic anhydride/polyvinyl alcohol/silk fibroin (COS-g-MAH/PVA/SF) composite and the results showed that the COS-g-MAH/PVA/SF composite has the effective biosorption for the removal of Pb(II) from aqueous solutions under pH 6 and contact time 180 min. Zhu et al. (2017) used the activable carboxylic acid to modify crystalline nanocellulose and then composited with PVA-co-PE to prepare CNC/PVA-co-PE nanofibrous membrane; the research indicated that the CNC/PVA-co-PE composite presented excellent selective adsorption on Cu(II) ions. Bozorgi et al. (2018) synthesized the PVA/chitosan/ZnO-NH_2 nanoadsorbents by casting and electrospinning methods respectively to remove the Cd(II) and Ni(II) from aqueous solution, and the results indicated that the Cd(II) ion presented a great inhibitory effect on Ni(II) adsorption in binary system.

The adsorption of PVA on heavy metal ions is a parallel process between the transmission of ion solution and formation of coordination bonds. Among which, the transmission of ion solution was related to the pore-channel structure while the formation of coordination bonds was associated with the adsorption groups. Most of the research was focused on the modification of functional groups or molecular structure to improve the adsorption capacity of adsorbent self merely. However, a non-negligible question was found in previous practical application that the pore structure of PVA gel was easily destroyed under surrounding's stress which will affect the real transmission and adsorption of ion solution. Thus, in this work, the inorganic ZnO whiskers modified by APTES were in situ introduced into the PVA matrix to steady the pore structure. The effect of ZnO morphological structure on the pore channel of PVA materials was researched with ordi-ZnO, nano-ZnO, and tetra-ZnO whiskers. The adsorption capacity and removal rate on Ni(II), Cd(II), Cr(III), and Pb(II) ions in a single-ion solution and mixed-ion solution were studied, respectively, and the adsorption mechanism was explored. Moreover, the stress stability, thermo stability, and reusability of PVA/ZnO composites were researched to investigate the feasibility in practical application.

Materials and methods

Materials

The PVA (1750 ± 50), boric acid (H_3BO_3), 3-triethoxysilylpropylamine (APTES), cadmium chloride ($CdCl_2$), chromium chloride ($CrCl_3$), nickel chloride ($NiCl_2$), lead nitrate ($Pb(NO_3)_2$), and calcium chloride ($CaCl_2$) were supplied by Sinopharm Chemical Reagent Co., Ltd. The ordi-ZnO was purchased from Xilong Scientific Co., Ltd., the nano-ZnO was purchased from Shanghai Aladdin Bio-Chem Technology Co., Ltd. and the tetra-ZnO was purchased from Chengdu Crystrealm Co., Ltd. Other chemical agents were all of analytic purity and used as received.

Synthesis and preparation

Modification of ZnO whiskers with APTES

The 10 g ZnO whiskers were dispersed in 200-mL toluene under ultrasound for 30 min, and then, 10 g APTES was added at 70 °C and stirred for 12 h. Finally, the mixed solution was filtered and the residue was washed by ethanol and then, the APTES-ZnO whiskers were obtained after drying.

Preparation of PVA/ZnO composites

PVA (5 g) and APTES-ZnO whiskers (0.5 g) with different structures were completely dissolved in ultrapure water (50 mL) and then were dropped into a gently stirred saturated $CaCl_2$-boric acid solution by an injector and were kept for 2 h under 30 °C to form spherical composite gel. The obtained PVA/ZnO composites were finally washed with ultrapure water and stored for further use after freeze drying.

Methods

FTIR analysis

The structure analysis of modified ZnO whiskers was conducted with a Nicolet-560 Fourier-transform infrared spectrometer (FTIR) (USA). The scanning rate was 20 min^{-1}, and the differential rate was 4 cm^{-1}.

SEM and EDS analysis

The micro morphology of modified ZnO whiskers and PVA/ZnO composites was observed through a JEOL JSM-5900LV scanning electron microscope (SEM) (Japan). The element composition of the materials was further analyzed with energy disperse spectroscopy (EDS).

TG analysis

The thermo-gravimetric analysis (TGA) of APTES-ZnO whiskers and PVA/ZnO composite was performed with a TA2950 thermo balance from TA Instruments Co. (USA) under nitrogen atmosphere with a heating rate of 10 °C/min. The test samples of about 10 mg were heated from ambient temperature to 800 °C.

Adsorption experiment of Ni(II), Cd(II), Cr(III), and Pb(II) ions

Adsorption in single heavy metal ion solution The adsorption experiment of different single heavy metal ions was performed according to the batch method. The conical flask containing of 0.3 g different PVA/ZnO composites and 100 mL different single heavy metal ion solutions (the initial concentration was 300 mg/L, pH was 5.0) were thermostatically vibrated at 25 °C for 24 h. Then, the PVA/ZnO composites were separated from the heavy metal ion solution, and the initial and final concentration of heavy metal ion solution was detected by ICP-OES (Agilent5100, USA). The equilibrium adsorption capacity (q_e) and removal rate (%) of the PVA/ZnO composites were calculated by the following expression, respectively (Vilela et al. 2018):

$$q_e = (C_i - C_e) \, V/M \qquad (1)$$

$$\text{removal rate } (\%) = (C_i - C_e) \times 100/C_i \qquad (2)$$

where q_e is the equilibrium adsorption capacity of unit mass PVA/ZnO composites; C_i and C_e are the initial and equilibrium concentrations of heavy metal ion solution, respectively; V is the volume of heavy metal ion solution, and M is the mass of dry PVA/ZnO composites.

Adsorption in mixed heavy metal ion solution

The mixed heavy metal ion solution was prepared with the mix of Ni(II), Cd(II), Cr(III), and Pb(II) ions (each one was 300 mg/L). The specific adsorption process and calculation method were the same as the adsorption experiment of single heavy metal ion solution.

Results and discussion

Modification mechanism and structure analysis of APTES-ZnO whiskers

In order to improve the interface compatibility between inorganic-organic phases, the different pure ZnO whiskers were coupling modified by APTES to graft the organics (Fig. 1(a)). The alkoxy groups of APTES hydrolyzed to give silanol groups and then reacted with the hydroxyl on ZnO whisker surface via dehydration to form Zn–O–Si bonds. And then, the structure was observed through FTIR spectra (Fig. 1(b)), the spectra of three kinds of neat ZnO whiskers were the same in spite of their different structures. After the modification by APTES, an obviously new absorption peak at 1008.4 cm^{-1} appeared which was attributed to the stretching vibration absorption of Si–O–Zn bond. Besides, the absorption peak intensity at 2923.2 cm^{-1} and 2853.7 cm^{-1} attributing to the stretching vibration absorption of —CH$_2$—showed a dramatical increase. Similarly, the absorption peak intensity at 3438.4 cm^{-1} attributing to the absorption of Zn–OH or –NH$_2$ increased also. The FTIR spectra indicated that the APTES successfully grafted onto the surface of ZnO whiskers.

The TGA was further used to evaluate the grafting rate of APTES on the surface of modified ZnO whiskers (Fig. 1(c)). The range between 250 °C and the end was attributed to the loss of grafted APTES organics. Thus, based on the results, the grafting rates of APTES for ordi-ZnO, nano-ZnO, and tetra-ZnO whiskers were 1.32%, 2.89% and 0.61%, respectively.

The micrographs of different ZnO whiskers before and after modification were observed through a SEM in Fig. 2. The ordi-ZnO and nano-ZnO presented the structure with irregular granules while that of tetra-ZnO was very regularly three-dimensional tetrapod-shaped whiskers. In terms of the whisker's size, the dimension of ordi-ZnO was about 1 μm and that of nano-ZnO was about 100 nm. However, the size of tetra-ZnO was relatively big with about 40 μm in length of the needle whisker and about 0.5 μm in diameter at the base. It was clearly seen that the three kinds of pure ZnO whiskers were seriously conglomerated before modification no matter its size or shape (Fig. 2(a, c, e)), and this phenomenon got obviously improved after modification (Fig. 2(b, d, f)).

Preparation of PVA/ZnO composites

The preparation of PVA/ZnO composites was proceed in a mixed matrix of PVA and ZnO whiskers with the H$_3$BO$_3$ and CaCl$_2$ as a cross-linking agent. In this in situ cross-linking process, the condensation reaction conducted between the hydroxyl of PVA molecular chains and boric acid. At the same time, the hydroxyl on the surface of ZnO whiskers reacted with the boric acid and the coordination between Ca(II) and hydroxyl was formed simultaneously. After the in situ cross-linking reaction, the dispersive PVA linear molecular chains connected together and the three-dimensional porous network structure was formed. The ZnO whiskers dispersed in the PVA network evenly with covalent bond and that the tetra-ZnO whiskers distributed in pore wall built a framework support structure due to the lap scarf effect of three-dimensional whisker arms of tetra-ZnO. The schematic of cross-linking reaction for PVA/tetra-ZnO composites is simulated in Fig. 3.
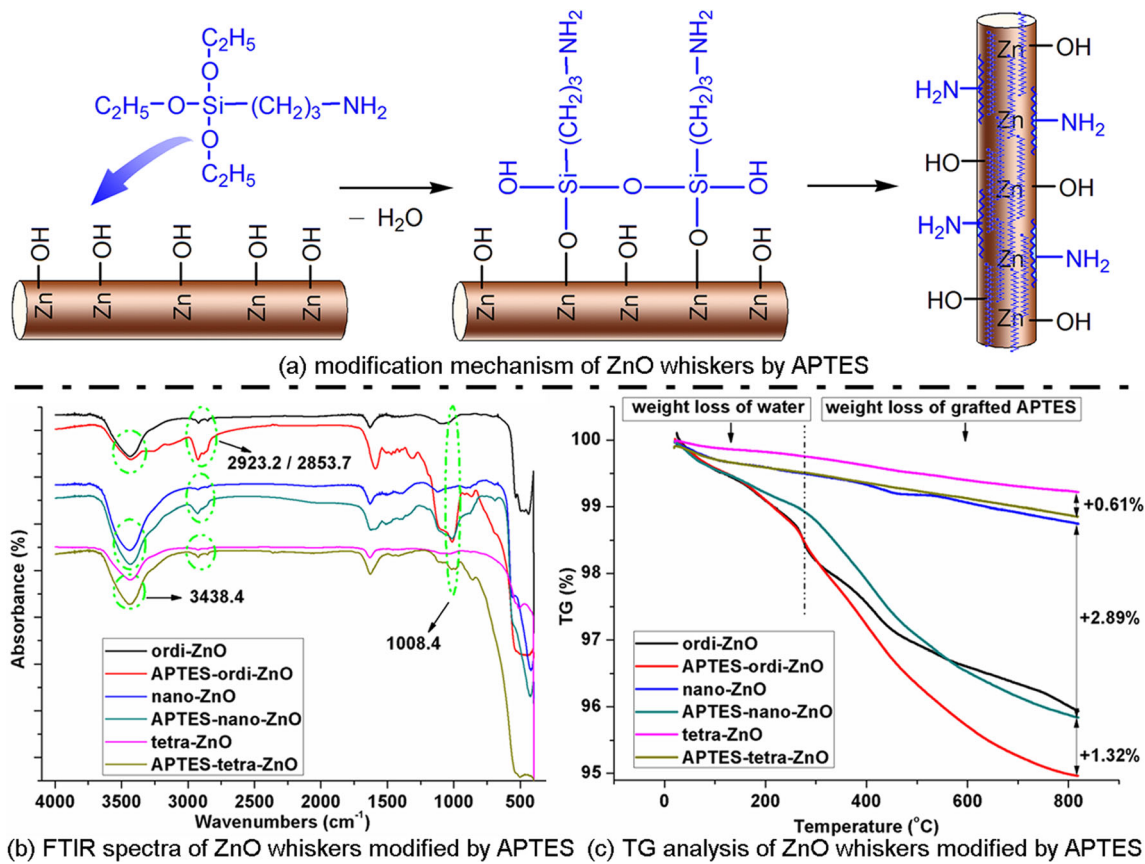
(a) modification mechanism of ZnO whiskers by APTES

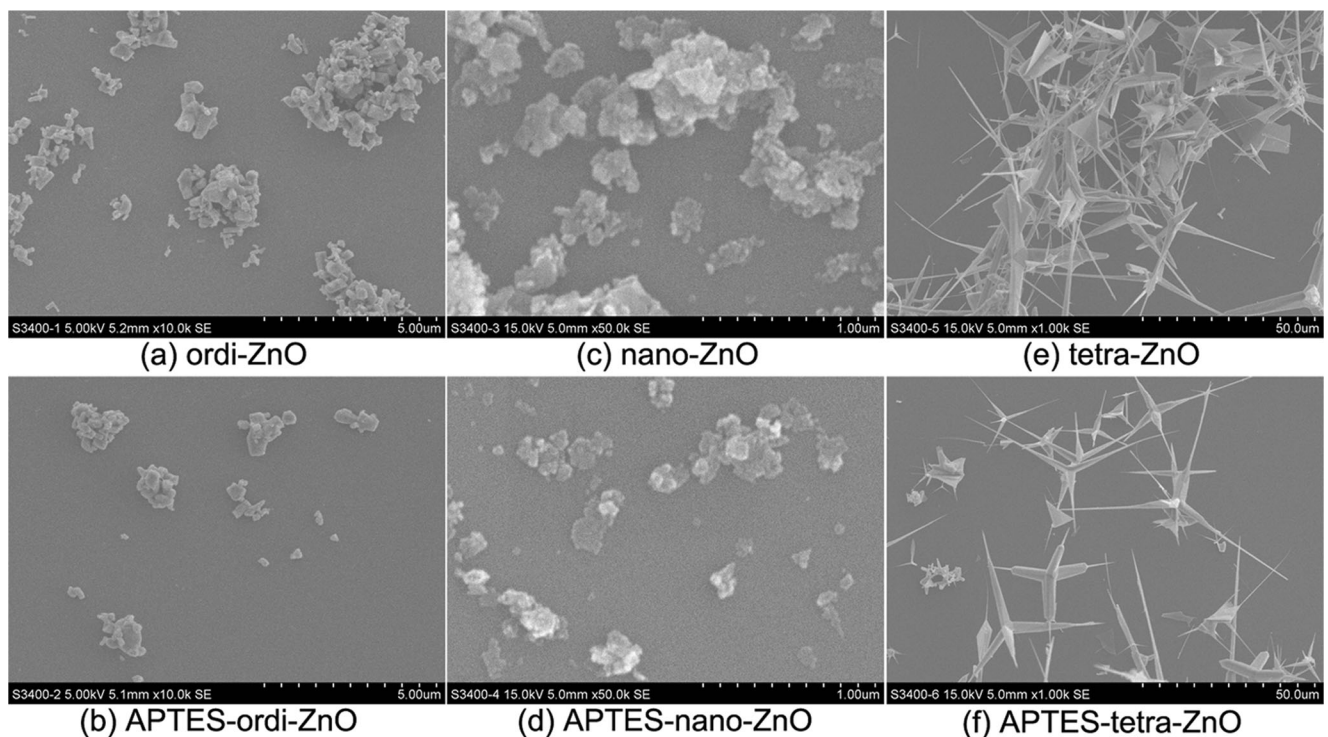(b) FTIR spectra of ZnO whiskers modified by APTES (c) TG analysis of ZnO whiskers modified by APTES

Fig. 1 Modification mechanism of ZnO whiskers by APTES and structure analysis

(a) ordi-ZnO   (c) nano-ZnO   (e) tetra-ZnO

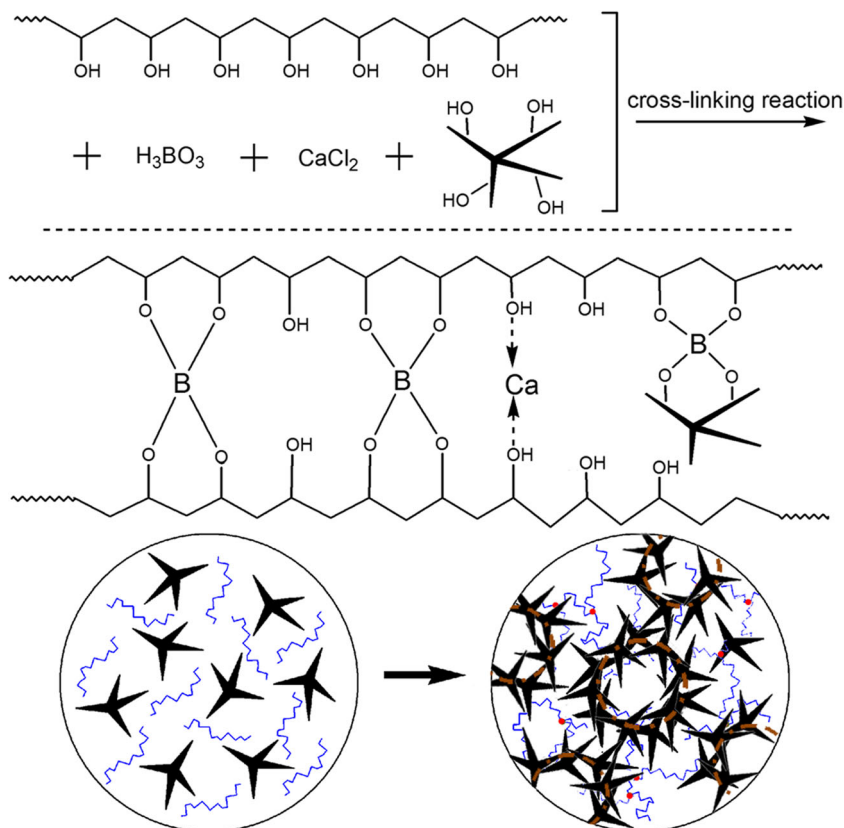(b) APTES-ordi-ZnO   (d) APTES-nano-ZnO   (f) APTES-tetra-ZnO

Fig. 2 SEM micrographs of different ZnO whiskers before and after coupling modification

Fig. 3 Schematic of cross-linking reaction for PVA/ZnO composites

Adsorption of heavy metal ion with different PVA/ZnO composites

The adsorption experiment on single and mixed heavy metal ions for different PVA/ZnO composites was conducted, respectively. As seen in the single adsorption in Fig. 4(a), all the PVA/ZnO composites showed a high adsorption capacity on Pb(II) and also showed a sub-high adsorption capacity on Cd(II) and Cr(III). However, the adsorption on Ni(II) was unsatisfactory for all kinds of PVA/ZnO composites. Comprehensive analysis, the neat PVA showed a not very strong adsorption performance on heavy metal ions except for the Pb(II). But this deficiency improved with the introduction of the ZnO whiskers. Among the three kinds of PVA/ZnO
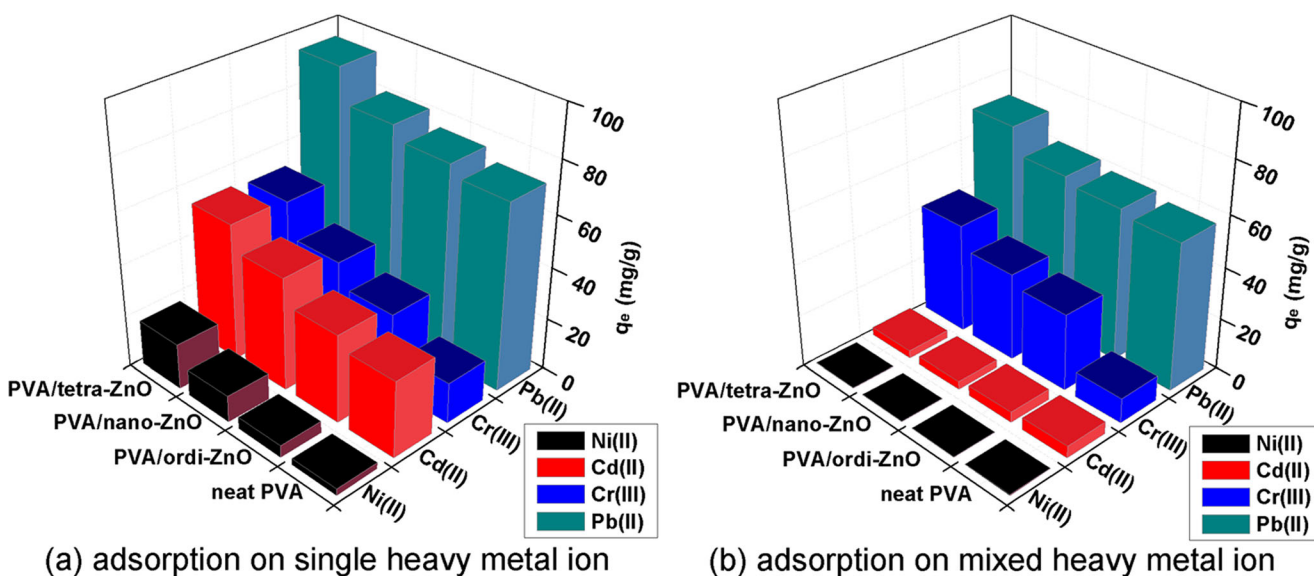

(a) adsorption on single heavy metal ion

(b) adsorption on mixed heavy metal ion

Fig. 4 Adsorption capacities of heavy metal ions with different PVA/ZnO composites

composites, the PVA/tetra-ZnO composite presented the biggest adsorption performance on heavy metal ions and the removal rate reached to 98%. The adsorption performance of PVA/nano-ZnO composites was better than that of PVA/ordi-ZnO composites which may result to a large number of the active adsorption group on the big specific surface of nano-ZnO whiskers.

The heavy metal ions in polluted water usually existed in mixture. It is necessary to study the adsorption performance of PVA/ZnO composites on mixed heavy metal ions. It can be visibly seen in Fig. 4(b) that the presence of mixed heavy metal ions strongly affected the adsorption and removal of heavy metal ions. Compared with the single adsorption, the mixed adsorption has shown a little decrease in different levels due to the competitive adsorption of mixed heavy metal ion solution. Even so, the adsorbent still maintained a higher adsorption capacity on Pb(II) than the other ions. Besides, the PVA/ZnO composites showed a sub-high adsorption on Cr(III) while that on Cd(II) decreased dramatically. Among the PVA/ZnO composites, the PVA/tetra-ZnO composites still showed a better adsorption performance than others. The

result indicated that the PVA/tetra-ZnO composite presented some selective adsorption characteristic in mixed heavy metal ion solution.

An important message can be obtained from Fig. 4 that the PVA/tetra-ZnO composite presented the best adsorption performance than other kinds of PVA/ZnO composites no matter single or mixed adsorption. This may relate to the internal micro pore-channel structure of PVA/ZnO composites. Therefore, the micro pore-channel structure of adsorbent was further observed in Fig. 5. At the same region, the pore-channel size was different among the PVA/ZnO composites and was obviously bigger than that of neat PVA material. The big size of pore-channel was beneficial for the transmission and diffusion of heavy metal ions and thus promoted the adsorption performance. Besides, the pore-channel structure of PVA/tetra-ZnO composites was more special. It can be clearly seen in Fig. 5(a–c) that the pores' wall for neat PVA or PVA/ordi-ZnO composites or PVA/nano-ZnO composites was very smooth and the adsorption behavior just conducted on the place of the pores' wall. But that of PVA/tetra-ZnO composites was rough and many agnail-like tetra-ZnO whiskers
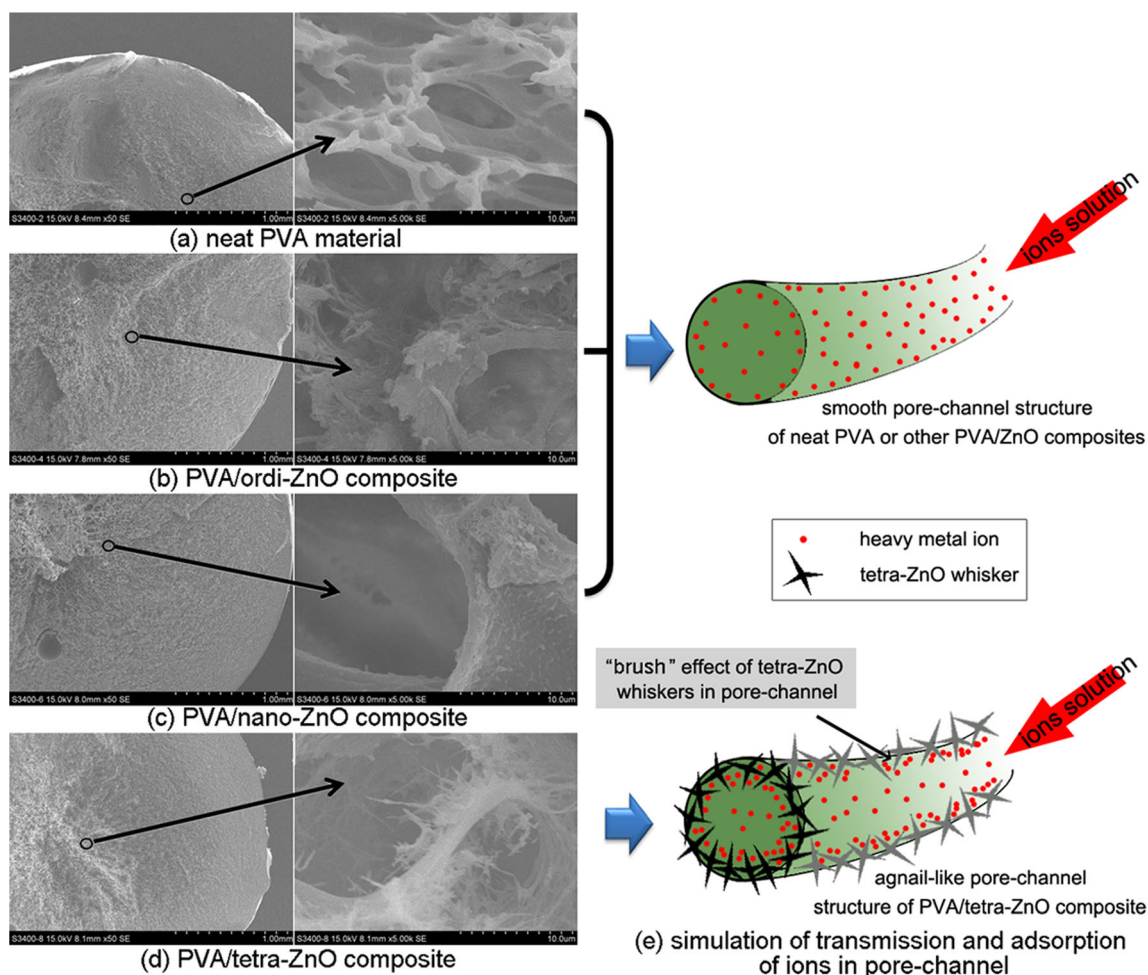

Fig. 5 SEM micrographs of different PVA/ZnO composites

existed in the pores' wall which will dramatically increase the adsorption area as seen in Fig. 5(d). Furthermore, the three-dimensional tetrapod-shaped ZnO whisker distributed in the pore's wall was easy to form a framework support structure which was beneficial for the transmission and adsorption of heavy metal ion. Besides, the agnail-like tetra-ZnO whiskers in the pores' wall will play as a "brush" which can effectively retain and capture the heavy metal ions when the ion solutions flow through the pore channel as simulated in Fig. 5(e)). Therefore, the PVA/tetra-ZnO composites showed better adsorption performance than the other kinds of PVA/ZnO composites.

Adsorption influence factor on Pb(II)

In consideration of the best adsorption performance of PVA/tetra-ZnO composite presented on Pb(II), the adsorption influence factor on Pb(II) was researched.

Adsorption isotherm

The equilibrium adsorption capacity q_e was dramatically influenced by initial concentration of heavy metal ions due to

the driving force of transmission between the solution and solid phases. As shown in Fig. 6(a), the q_e of the PVA/tetra-ZnO composite increased gradually with the increasing initial Pb(II) concentration and showed a higher than 90% removal rate in the range of 0~300 mg/L initial concentration. With the increasing concentration of metal ions, the q_e tended to be stable at about 400 mg/L initial concentration and the maximal adsorption capacity q_m obtained from experiment was about 112.64 mg/g under the current conditions.

The Langmuir model, Freundlich model, and Temkin model were used to analyze the Pb(II) adsorption mechanism. The Langmuir model assumes that adsorption occurs on homogeneous surface by monolayer adsorption, and the Freundlich model is used to describe the multilayer adsorption onto the surface of heterogeneous sites, while the Temkin model assumes that the adsorption heat decreases linearly rather than logarithmically and its adsorption is uniformly distributed (Zhang et al. 2010). The equations of the three adsorption isotherm models are expressed as follows:

$$Langmuir\ model\ q_e = \frac{K_l q_m C_e}{1 + K_l C_e} \quad (3)$$

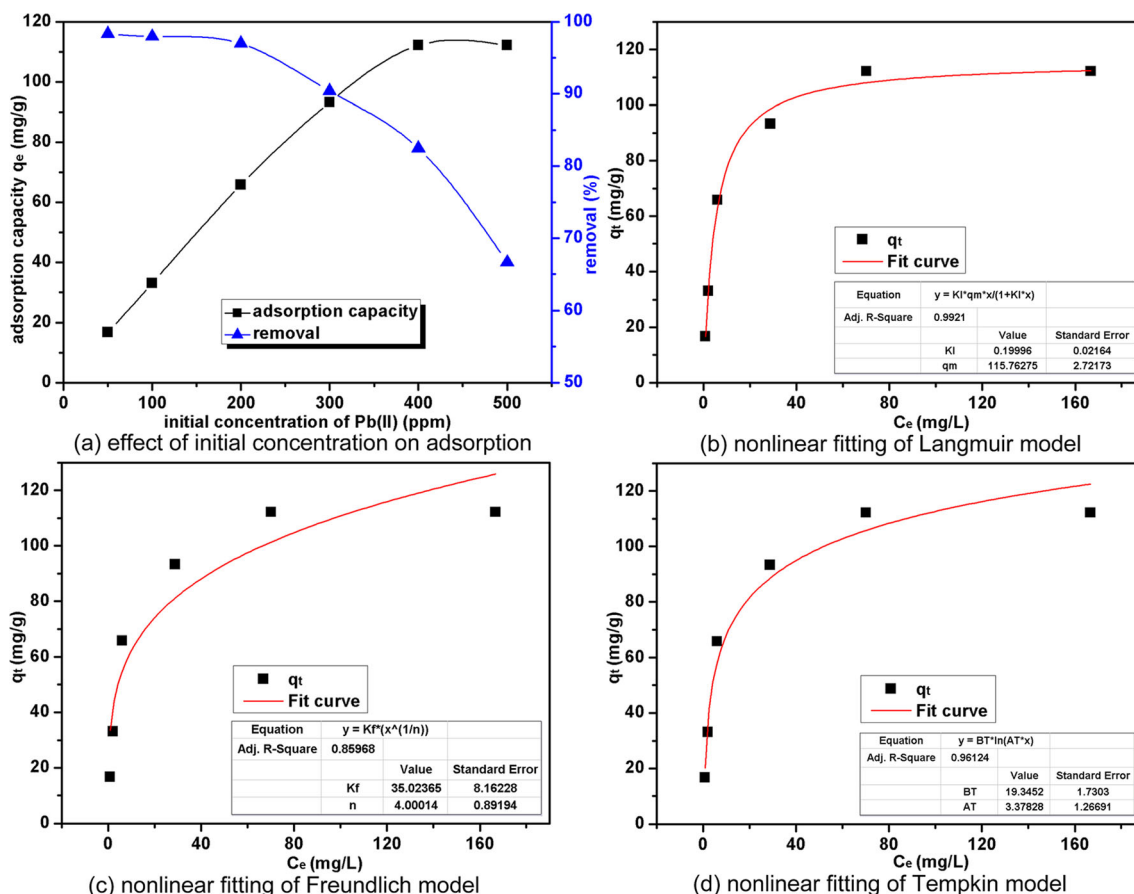$$Freundlich\ model\ q_e = K_f C_e^{\frac{1}{n}} \quad (4)$$

Fig. 6 Effect of initial concentration on adsorption and nonlinear fitting of adsorption isotherm models for PVA/tetra-ZnO composites

Table 1 Isotherm parameters of the Pb(II) adsorption for PVA/tetra-ZnO composite

Adsorption isotherm	Adsorption isotherm parameters		R^2
Langmuir model	q_m (mg/g)	115.76	0.9921
	K_l (L/mg)	0.20	
Freundlich model	K_f ((mg/g)(L/mg)$^{1/n}$)	35.02	0.8597
	n	4.00	
Temkin model	A_T (L/mg)	3.38	0.9612
	b_T ((g/mg)(J/mol))	128.10	

$$Temkin\ model\ q_e = (RT/b_T)\ln(A_T C_e) \quad (5)$$

where q_e is the adsorption capacity at equilibrium; C_e is the solution concentration at equilibrium; q_m is the maximum adsorption capacity, and K_l is the Langmuir coefficient related to the affinity of the binding site. K_f and n are the constants related to the adsorption capacity and the adsorption intensity, respectively. A_T is the equilibrium binding constant corresponded to the maximum binding energy, and b_T is the constant related to the adsorption heat.

The nonlinear plots of q_e versus C_e of the PVA/tetra-ZnO composite are shown in Fig. 6(b–d) according to Eqs.3–5,

respectively. The isotherm parameters are obtained and listed in Table 1. It can be seen that the value of correlation coefficient (R^2) for the Langmuir model was 0.9921 which was bigger than that for Freundlich model ($R^2 = 0.8597$). And the q_m obtained from the modeling of isotherm was 115.76 mg/g which was very close to the q_m obtained from the experiment. The result indicated that the Langmuir model was more suitable to represent the equilibrium data than the Freundlich model and the Pb(II) adsorption of PVA/tetra-ZnO composite was a homogeneous monolayer adsorption. Besides, the R^2 for the Temkin model was 0.9612 which represented a good fitting. The big value of b_T indicated the considerable potential of PVA/tetra-ZnO composite in the application of Pb(II) removal.

Adsorption kinetics

The adsorption performance of PVA/tetra-ZnO composite was affected by contact time as well and the correlation curve between contact time and adsorption capacity is shown in Fig. 7(a). It can be seen that the adsorption capacity and removal rate increased quickly with time and then a slow stage appeared until the matrix reached to an equilibrium state. In order to further understand the kinetic characteristics of the Pb(II) adsorption process for PVA/tetra-ZnO composite, the
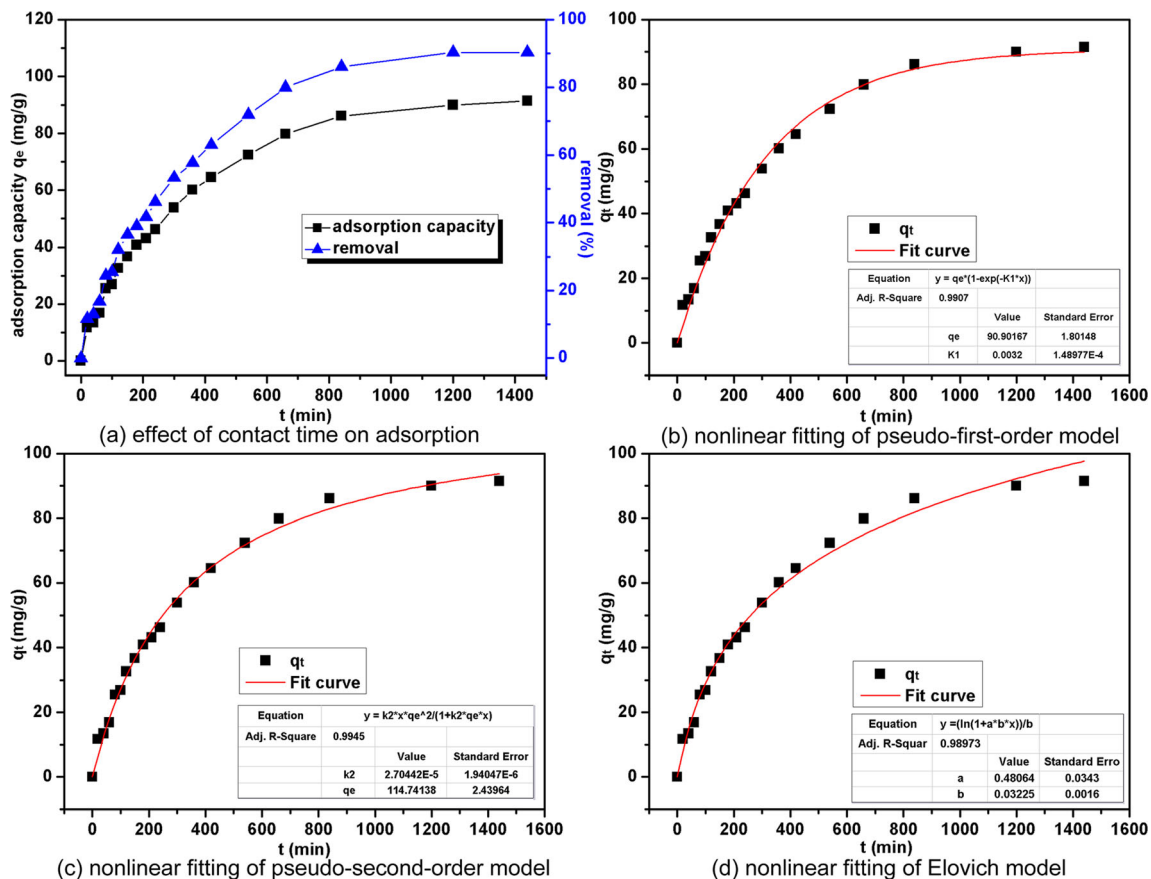

Fig. 7 Effect of contact time on adsorption and nonlinear fitting of adsorption kinetics models for PVA/tetra-ZnO composites

Table 2 Kinetic parameters of the Pb(II) adsorption for PVA/tetra-ZnO composite

Adsorption kinetics	Adsorption kinetic parameters		R^2
pseudo-first-order model	k_1 (1/min)	3.20×10^{-3}	0.9907
	q_e (mg/g)	90.90	
pseudo-second-order model	k_2 (g/(mg min))	2.70×10^{-5}	0.9945
	q_e (mg/g)	114.74	
Elovich model	a (mg/(g·min))	0.481	0.9897
	b (g/mg)	0.032	

Lagergren pseudo-first-order model, Ho-McKay pseudo-second-order model, and Elovich model (Denys et al. 2018) were used to examine the rate-controlling mechanism. The three adsorption kinetics equations are given as follows:

$$pseudo-first-order\ model\quad q_t = q_e\left(1 - e^{-k_1 t}\right) \tag{6}$$

$$pseudo-second-order model\quad q_t = \frac{k_2 q_e^2 t}{1 + k_2 q_e t} \tag{7}$$

$$Elovich\ model\quad q_t = \frac{1}{b}\ln(1 + abt) \tag{8}$$

where q_e is the adsorption capacity at equilibrium; q_t is the adsorption capacity at time t; k_1 is the rate constant of pseudo-first-order adsorption, and k_2 is the rate constant of pseudo-second-order adsorption. The parameter a is the initial adsorption rate of the Elovich model and b is the desorption constant related to the extent of the surface coverage and activation energy for chemisorption.

The nonlinear plots of q_t versus t of the PVA/tetra-ZnO composite are shown in Fig. 7(b–d) according to Eqs.6–8, respectively. The kinetic parameters are obtained and listed in Table 2. The pseudo-first-order model assumed that the adsorption process was a diffusion-controlled step while the pseudo-second-order model was used to describe the chemical adsorption-controlled step. It can be seen that the pseudo-second-order model presented

the better fitting degree than that of the pseudo-first-order model and showed a higher correlation coefficient ($R^2 = 0.9945$). And besides, the adsorption capacity at equilibrium obtained by nonlinear fitting of the pseudo-second-order model is about 114.74 mg/g which is near to the experiment result. Thus, it can be concluded that the Pb(II) adsorption process of PVA/tetra-ZnO composite was controlled by the chemical adsorption. However, the diffusion process also played a non-negligible role due to it sub-high correlation coefficient ($R^2 = 0.9907$). Besides, the correlation coefficient of the Elovich model was up to 0.9897, indicative of the predominant chemical nature of Pb(II) adsorption on PVA/tetra-ZnO composite.

Adsorption thermodynamics

The adsorption process was also affected by the matrix temperature as seen in Fig. 8(a). With the increasing solution temperature, the adsorption capacity and removal rate increased gradually. The result indicated that the high temperature was favorable for the Pb(II) adsorption process of PVA/tetra-ZnO composite. Thermodynamic parameters can be determined by the equilibrium constant K^θ which is equal to $\rho \times q_e/C_e$ (ρ is the water density and $\rho = 1000$ g/L) and depends on the temperature (Slobodan 2007; Nasseh et al. 2019). The change of Gibbs free energy (ΔG^θ), enthalpy (ΔH^θ), and entropy (ΔS^θ) associated with the adsorption process was calculated by the following equations.

$$K^\theta = \exp\left(\frac{\Delta S^\theta}{R} - \frac{\Delta H^\theta}{RT}\right) \tag{9}$$

$$\Delta G^\theta = \Delta H^\theta - T\Delta S^\theta \tag{10}$$

where R is the ideal gas constant and equal to 8.314 J/mol K; T is the solution temperature. The nonlinear fitting curve between K^θ and T was plotted according to Eq. 9 and was shown in Fig. 8(b). And then, the thermodynamic parameters were obtained and listed in Table 3.
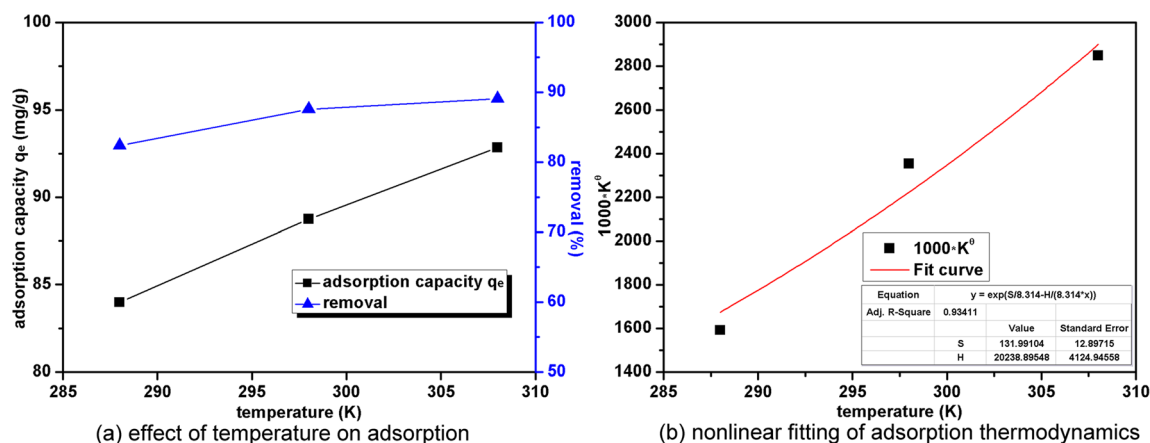

Fig. 8 Effect of temperature on adsorption and nonlinear fitting of adsorption thermodynamics for PVA/tetra-ZnO composites

Table 3 Thermodynamic parameters of the Pb(II) adsorption for PVA/tetra-ZnO composite

Temperature (K)	K^{θ}	ΔG^{θ} (kJ/mol)	ΔH^{θ} (kJ/mol)	ΔS^{θ} (J/mol·K)	R^2
288	1591	− 17.77	20.239	131.99	0.9341
298	2353	− 19.09			
308	2848	− 20.41			

It is clearly seen that the positive value of ΔH^{θ} indicated the endothermic nature of the adsorption process and the positive value of ΔS^{θ} suggested an increasing disorderliness at the solid-solution interface for the Pb(II) adsorption onto the PVA/tetra-ZnO composite. The values of ΔG^{θ} were negative within the test temperature range, indicating that the adsorption process of PVA/tetra-ZnO composite on Pb(II) was spontaneous. In addition, with the increasing temperature from 288 to 308 K, the value of ΔG^{θ} shifted from − 17.77 to − 20.41 kJ/mol. The decrease of ΔG^{θ} indicated that the adsorption process was favorable at high temperatures.

Exploring adsorption mechanism

The adsorption mechanism of adsorbing material on Pb(II) has been studied by SEM-EDS as shown in Fig. 9(a, b). The content of Ca element on the surface layer dramatically decreased from 5.20% before adsorption to 0.28% after adsorption. The

decrease of Ca content indicated that the ion exchange between the Ca(II) and Pb(II) occurred during the adsorption process. Except this, the adsorption behavior occurred because of the formation of coordination bonds between the –OH, –NH$_2$ etc. group and the heavy metal ions which has been widely acknowledged. In terms of our adsorbent, the coordination bonds formed between the –OH in PVA molecular chains or the –OH on the surface of ZnO whisker or the –NH$_2$ in grafted APTES with the Pb(II). Therefore, the adsorption mechanism of this PVA material on Pb(II) was conducted by the combined effect of coordination and ion exchange as simulated in Fig. 9(c).

Stability and reusability of PVA/tetra-ZnO composites

Stress stability

As to an excellent adsorbent, the materials should present well stress stability and applicability in true environment.

Element	Weight%	Atomic%
C	36.24	44.32
O	58.56	53.77
Ca	5.20	1.90

(a) element distribution before adsorption

Element	Weight%	Atomic%
C	48.26	58.93
O	44.13	40.45
Ca	0.28	0.10
Pb	7.33	0.52

(b) element distribution after adsorption
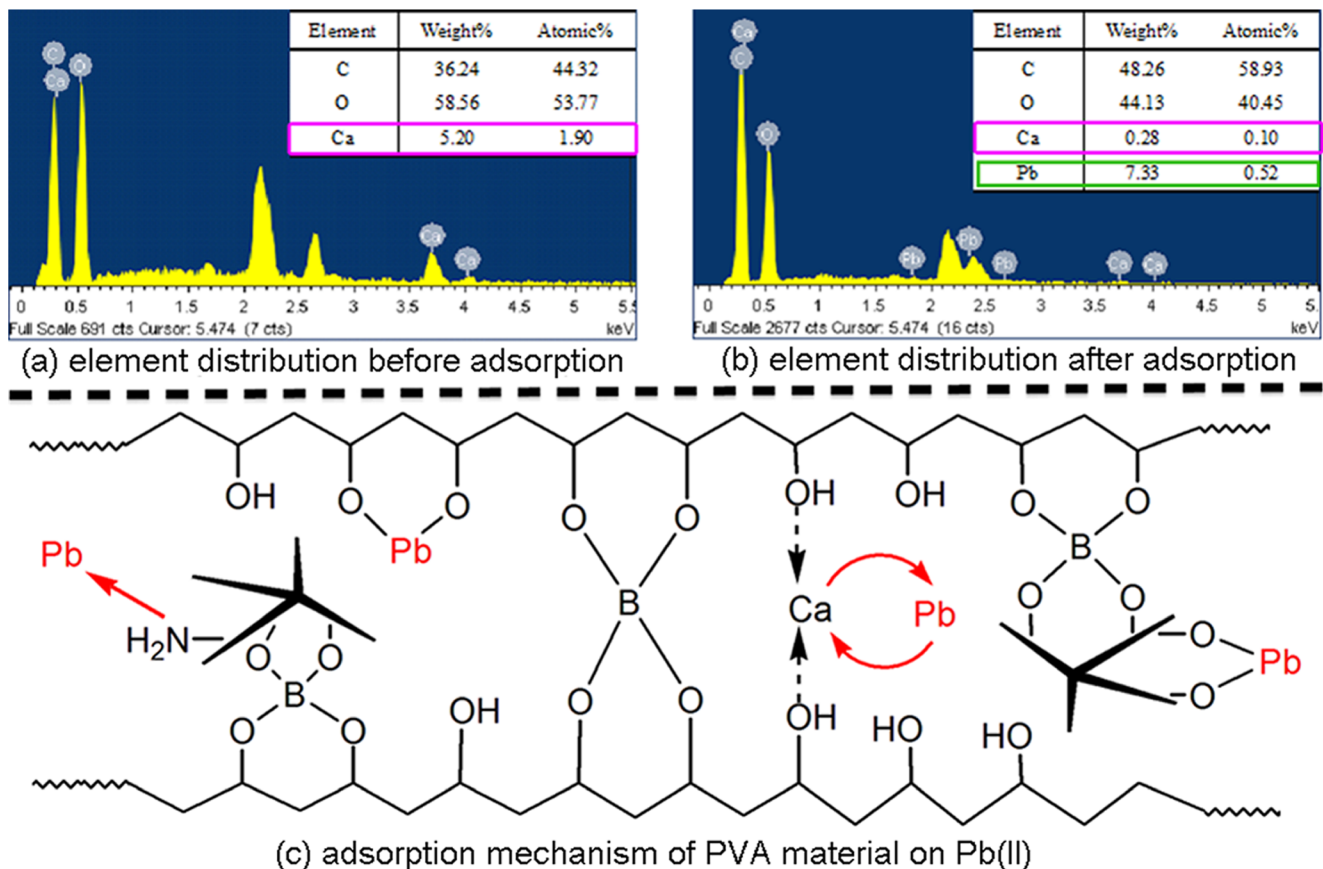
(c) adsorption mechanism of PVA material on Pb(II)

Fig. 9 Pb(II) adsorption mechanism in PVA material

However, the pore structure of neat PVA was destroyed evidently as shown in Fig. 10(a). The pore structure in the out layer was compressed and collapsed and that in the inner layer was even compacted without any pore structure. Consequently, the adsorbed Pb(II) majorly distributed around the out layer of neat PVA materials and no content was detected in the core region. However, this circumstance got improved vastly after the introduction of tetra-ZnO (Fig. 10(b)). Under the same external stress, the pore channel still kept the typical pore structures no matter the out or inner layer. Meanwhile, the adsorbed Pb(II) was not only majorly distributed in out layer but also a certain content of Pb(II) was detected in the core region. The result indicated that the formation of framework-supported pore-channel structure due to the

three-dimensional tetrapod-shaped ZnO whiskers was in favor of the transmission and adsorption of heavy metal ions under external stress in practical application.

Thermo stability

The thermo stability of different PVA/ZnO composites was evaluated as shown in Fig. 11(a). With the increase of temperature, the mass decreased gradually due to the volatilization of micromolecule and decomposition of polymer. The process of mass loss can be divided into three stages. Among which, the second stage from 260 to 390 °C was attributed to the loss of hydroxyl in PVA molecular chains. And then, the last stage from 390 °C to the end was ascribed to the breakage and decomposition
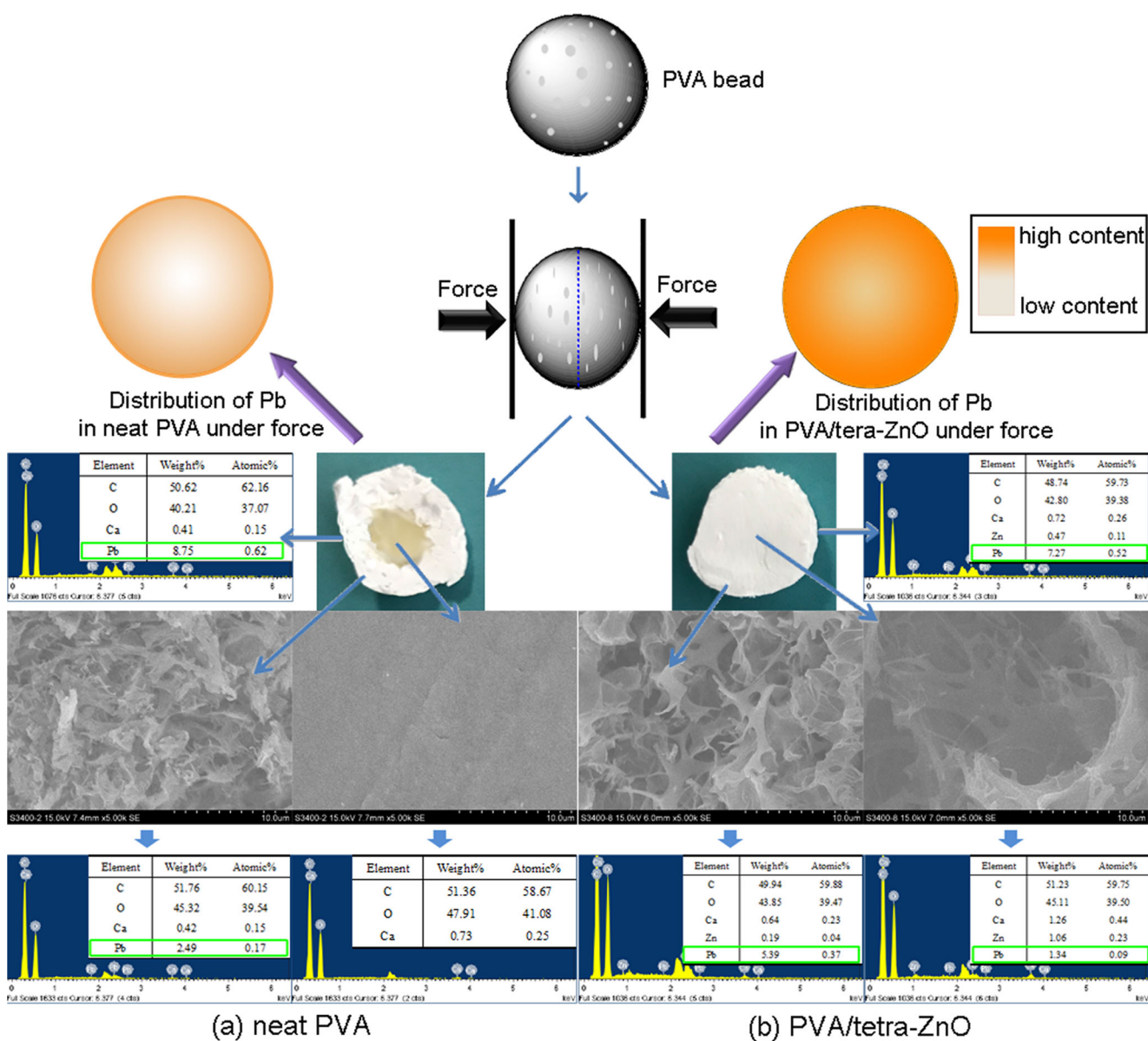

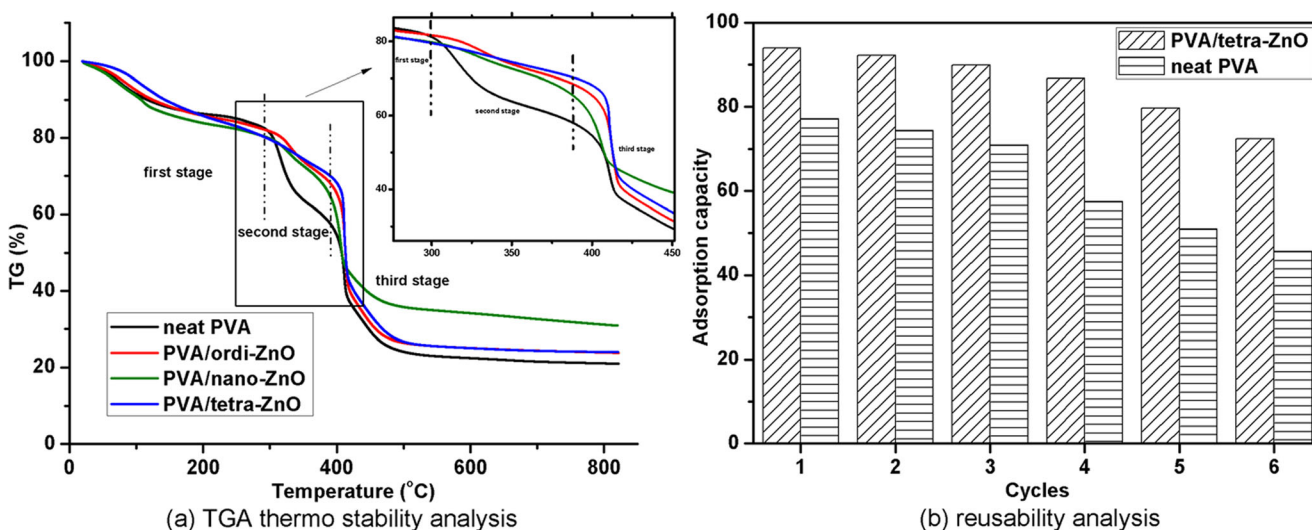**Fig. 10** Steady pore structure of PVA/tetra-ZnO adsorbent under stress

Fig. 11 Thermo stability and reusability analysis of PVA/ZnO composites

of PVA polymer. By the introduction of ZnO whiskers, the initial decomposition temperature of the second stage and third stage was increased by 35 °C and 20 °C, respectively. Besides, the second stage of neat PVA material was very obvious while that of PVA/ZnO composites was unapparent. The results indicated that the thermo stability of PVA adsorbent was improved dramatically after the introduction of ZnO whiskers.

Reusability

The reusability of adsorbent should be considered to evaluate the economic feasibility. Thus, the adsorption-desorption experiment of PVA/tetra-ZnO composites on Pb(II) was investigated up to six cycles as seen in Fig. 11(b). It can be seen that the adsorption capacity of Pb(II) is relatively stable within the four cycles without an obvious decrease. With the further increase of cycles, the adsorption performance of Pb(II) still maintained a high level, although the adsorption capacity showed a little decrease in value. As a comparison, the adsorption capacity of neat PVA began to dramatically decrease after the third cycle of adsorption-desorption processes. Thus, it can be concluded that the PVA/tetra-ZnO composites have a good reusability and considerable potential in the application of heavy metal ion removal.

Conclusions

The PVA/ZnO composites were prepared by in situ cross-linking reaction and the effect of ordi-ZnO, nano-ZnO, and tetra-ZnO whiskers structure on the micro pore channel was studied. The results showed that the tetra-ZnO whisker was beneficial for the formation of "framework support"

structure macro-pores due to the long and three-dimensional whiskers and which was in favor of the transmission of heavy metal ion solution. Among the composites with different ZnO whiskers, the PVA/tetra-ZnO composites presented the best adsorption performance on single heavy metal ions than others and as well as the selective adsorption on mixed heavy metal ions, especially on the Pb(II) and Cr(III) ions. The tetra-ZnO whiskers stabbed in the pore wall-like agnail acted as a "brush" which will effectively retain and capture the heavy metal ions when the ion solutions flow through the pore channel. The adsorption process was fitted well to the Langmuir model and the adsorption kinetics was in accordance with the pseudo-second-order model due to the chemical adsorption-controlled step. The adsorption process was spontaneous and the high temperature was in favor of adsorption. The adsorption mechanism was studied as the combination of coordination and ion exchange. Moreover, the PVA/tetra-ZnO composites presented a good transmission and adsorption of heavy metal ions under external stress due to the formation of "framework support" pore-channel structure. The thermo stability of PVA/tetra-ZnO composites was dramatically improved and the PVA/tetra-ZnO composites exhibited favorable reusability within five cycles without a big decrease in adsorption performance on heavy metal ions.

Compliance with ethical standards

Conflict of interest The authors declare that they have no conflict of interest.

References

Abdullah NH, Shameli K, Abdullah EC, Abdullah LC (2019) Solid matrices for fabrication of magnetic iron oxide nanocomposites: synthesis, properties, and application for the adsorption of heavy metal ions and dyes. Compos Part B-Eng 162:538–568

Ahmed MB, Zhou JL, Ngo HH, Guo WS, Thomaidis NS, Xu J (2017) Progress in the biological and chemical treatment technologies for emerging contaminant removal from wastewater: a critical review. J Hazard Mater 323:274–298

Sarma GK, Gupta SS, Bhattacharyya KG (2019) Nanomaterials as versatile adsorbents for heavy metal ions in water: a review. Environ Sci Pollut Res 26(7):6245–6278

Abdelrahman EA, Hegazey RM (2019) Exploitation of Egyptian insecticide cans in the fabrication of Si/Fe nanostructures and their chitosan polymer composites for the removal of Ni(II), Cu(II), and Zn(II) ions from aqueous solutions. Compos Part B-Eng 166:382–400

Tran HN, Chao HP (2018) Adsorption and desorption of potentially toxic metals on modified biosorbents through new green grafting process. Environ Sci Pollut Res 25(13):12808–12820

Reddi MRG, Govindharajan C, Sudha PN, Gomathi T (2015) Adsorption studies on the removal of chromium onto chitosan-g-maliec anhydride-g-ethylene dimethacrylate. J Chem Pharm Res 7:467–476

Li ZT, Wang L, Meng J, Liu XM, Xu JM, Wang F, Brookes P (2018) Zeolite-supported nanoscale zero-valent iron: new findings on simultaneous adsorption of Cd(II), Pb(II), and As(III) in aqueous solution and soil. J Hazard Mater 344:1–11

Liu XJ, Lai DG, Wang Y (2019) Performance of Pb(II) removal by an activated carbon supported nanoscale zero-valent iron composite at ultralow iron content. J Hazard Mater 361:37–48

Arshad F, Selvaraj M, Zain J, Banat F, Haija MA (2019) Polyethylenimine modified graphene oxide hydrogel composite as an efficient adsorbent for heavy metal ions. Sep Purif Technol 209: 870–880

Huang Y, Zeng XF, Guo LL, Lan JH, Zhang LL, Cao DP (2018) Heavy metal ion removal of wastewater by zeolite-imidazolate frameworks. Sep Purif Technol 194:462–469

Ko D, Mines PD, Jakobsen MH, Yavuz CT, Hansen HCB, Andersen HR (2018) Disulfide polymer grafted porous carbon composites for heavy metal removal from stormwater runoff. Chem Eng J 348: 685–692

Dong LY, Jiao F, Qin WQ, Zhu HL, Jia WH (2019) Activation effect of lead ions on scheelite flotation: adsorption mechanism, AFM imaging and adsorption model. Sep Purif Technol 209:955–963

Chen L, Chen NN, Wu HM, Li WX, Fang Z, Xu ZW, Qian XM (2018) Flexible design of carbon nanotubes grown on carbon nanofibers by PECVD for enhanced Cr(VI) adsorption capacity. Sep Purif Technol 207:406–415

Zou CL, Jiang W, Liang JY, Sun XH, Guan YY (2019) Removal of Pb(II) from aqueous solutions by adsorption on magnetic bentonite. Environ Sci Pollut Res 26(2):1315–1322

Hayati B, Maleki A, Najafi F, Gharibi F, McKay G, Gupta VK, Puttaiah SH, Marzban N (2018) Heavy metal adsorption using PAMAM/CNT nanocomposite from aqueous solution in batch and continuous fixed bed systems. Chem Eng J 346:258–270

Hui B, Zhang Y, Ye L (2015) Structure of PVA/gelatin hydrogel beads and adsorption mechanism for advanced Pb(II) removal. J Ind Eng Chem 21:868–876

Ajitha P, Vijayalakshmi K, Saranya M, Gomathi T, Rani K, Sudha PN, Anil S (2017) Removal of toxic heavy metal lead (II) using chitosan oligosaccharide-graft-maleic anhydride/polyvinyl alcohol/silk fibroin composite. Int J Biol Macromol 104:1469–1482

Zhu Q, Wang Y, Li MF, Liu K, Hu CY, Yan KL, Sun G, Wang D (2017) Activable carboxylic acid functionalized crystalline nanocellulose/PVAco-PE composite nanofibrous membrane with enhanced adsorption for heavy metal ions. Sep Purif Technol 186:70–77

Bozorgi M, Abbasizadeh S, Samani F, Mousavi SE (2018) Performance of synthesized cast and electrospun PVA/chitosan/ZnO-NH$_2$ nanoadsorbents in single and simultaneous adsorption of cadmium and nickel ions from wastewater. Environ Sci Pollut Res 25(18):17457–17472

Vilela PB, Dalalibera A, Duminelli EC, Becegato VA, Paulino AT (2018) Adsorption and removal of chromium (VI) contained in aqueous solutions using a chitosan-based hydrogel. Environ Sci Pollut Res https://doi.org/10.1007/s11356-018-3208-3

Zhang Y, Li YF, Li XL, Yang LQ, Bai X, Ye ZF, Zhou LC, Wang LY (2010) Selective removal for Pb^{2+} in aqueous environment by using novel macroreticular PVA beads. J Hazard Mater 181:898–907

Denys ASR, Jaqueline MM, Guilherme LD, Tito RSC Jr, Luiz AAP (2018) Preparation, characterization and dye adsorption/reuse of chitosan-vanadate films. J Polym Environ 26:2917–2924

Slobodan KM (2007) A consideration of the correct calculation of thermodynamic parameters of adsorption. J Serb Chem Soc 72(12): 1363–1367

Nasseh N, Barikbin B, Taghavi L, Nasseri MA (2019) Adsorption of metronidazole antibiotic using a new magnetic nanocomposite from simulated wastewater (isotherm, kinetic and thermodynamic studies). Compos Part B-Eng 159:146–156